Formation of Lewis Acidic Support Materials via Chemisorption of Trimethylaluminum on Mesoporous Silicate MCM-41

Reiner Anwander,* Clemens Palm, Olaf Groeger, and Günter Engelhardt

Institut für Technische Chemie I, Universität Stuttgart, Pfaffenwaldring 55, D-70569 Stuttgart, Germany

Received December 3, 1997

The chemisorption of trimethylaluminum on dehydrated mesoporous MCM-41 is described. The sorption capacity of the silicate material was examined by addition of various amounts of the organoaluminum reagent and monitored by elemental analysis, FTIR spectroscopy, and nitrogen physisorption measurements. Multinuclear (^{1}H, ^{13}C, ^{27}Al) solid-state NMR studies reveal a methyl surface population with a $SiCH_3/AlCH_3$ ratio of approximately 0.45 and suggest a highly distorted geometry and polarized charge density, respectively, at the aluminum centers. Air-exposed samples indicate the formation of four- and six-coordinate aluminum. The $AlMe_3$-modified MCM-41 materials exhibit a strong Lewis acidic behavior, as derived from a novel "test reaction", involving an intermetallic Lewis acid-base competition reaction between the support system and the spectroscopically versatile, *n*-hexane-soluble complex $Y[N(SiHMe_2)_2]_3(THF)_2$. Additionally, the rare earth dimethylsilylamide reagent seems to be a promising probe molecule for examining the alkylation capability of such organoaluminum-modified support materials.

Introduction

Modification of chemically and thermally robust support materials such as silica, alumina, or zeolites via surface organometallic chemistry is a promising approach to generate supramolecular entities of relevance in both catalysis[1,2] and materials sciences.[3] Organoaluminum compounds, in particular the commercially available trimethylaluminum, were routinely utilized to manipulate silica surfaces as (i) H-sequestering agents for the quantification of surface silanol groups,[4] (ii) a source of alumina to generate catalytically active hybrid species (alumination reactions),[5] (iii) a passivating and/or compatibilizing agent for the immobilization of molecular precatalyst species,[6] and (iv) a (co)reactant to produce aluminum-containing thin-layer materials such as AlN.[7]

Recently, we envisaged mesoporous silicate MCM-41,[8,9] a structurally ordered modification of silica, as an intriguing platform to study surface organometallic reactions.[10] Surface areas higher than 1000 $m^2\ g^{-1}$ and a honeycomb structure of uniform mesopores ensure both a higher guest loading and a more detailed characterization by means of nitrogen adsorption/desorption, XRD, and HRTEM compared to the conventional silica support materials.[11] In particular, nitrogen physisorption measurements allow a unique picturing of the intraporous population by representation of the pore volume and the pore size distribution. Similar to the commonly used silica and alumina supports,[2] MCM-41 materials are capable of surface reactions via silanol groups and strained siloxane bridges. Only a few MCM-

* To whom correspondence should be addressed. Present address: Anorganisch-chemisches Institut, Technische Universität München, Lichtenbergstrasse 4, D-85747 Garching b. München, Germany. Telefax: Int. + 89-289-13473. E-mail: anwander@arthur.anorg.chemie.tu-muenchen.de.

(1) (a) Hartley, F. R.; Vezey, P. N. *Adv. Organomet. Chem.* **1977**, *15*, 189. (b) Bailey, D. C.; Langer, S. H. *Chem. Rev.* **1981**, *81*, 109. (c) Iwasawa, Y. *Adv. Catal.* **1987**, *35*, 187. Zechina, A.; Areán, C. O. *Catal. Rev.—Sci. Eng.* **1993**, *35*, 262. (d) *Surface Organometallic Chemistry, Molecular Approaches to Surface Catalysis*; Basset, J.-M., Gates, B. C., Candy, J. P., Choplin, A., Leconte, H., Quignard, F., Santini, C., Eds.; Kluwer: Dordrecht, 1988. (e) Marks, T. J. *Acc. Chem. Res.* **1992**, *25*, 57.

(2) (a) Robinson, A. L. *Science* **1976**, *194*, 1261. (b) Sachtler, W. M. H.; Zhang, Z. *Adv. Catal.* **1993**, *39*, 129. (c) Bein, T. In *Comprehensive Supramolecular Chemistry;* Alberti, G., Bein, T., Eds.; Elsevier: Oxford, 1996; Vol. 7, p 579.

(3) Stucky, G. D.; MacDougall, J. E. *Science* **1990**, *247*, 669. (b) Stucky, G. D. *Prog. Inorg. Chem.* **1992**, *40*, 99. (c) Ozin, G. A.; Özkar, S.; Prokopowicz, R. A. *Acc. Chem. Res.* **1992**, *25*, 553.

(4) (a) Liefländer, M.; Stöber, W. *Z. Naturforsch.* **1960**, *15B*, 411. (b) Sato, M.; Kanbayashi, T.; Kobayashi, N.; Shima, Y. *J. Catal.* **1967**, *7*, 342. (c) Kunawicz, J.; Jones, P.; Hockey, J. A. *Trans. Faraday Soc.* **1971**, *67*, 848. (d) Morrow, B. A.; McFarlan, A. J. *Langmuir* **1991**, *7*, 1695.

(5) (a) Murray, J.; Sharp, M. J.; Hockey, J. A. *J. Catal.* **1970**, *18*, 52. (b) Peglar, R. J.; Hambleton, F. H.; Hockey, J. A. *J. Catal.* **1971**, *20*, 309. (c) Hambleton, F. H.; Hockey, J. A. *J. Catal.* **1971**, *20*, 321. (d) de Ruiter, R.; Jansen, J. C.; van Bekkum, H. In *Molecular Sieves*; Occelli, M. L., Robson, H. E., Eds.; Van Nostrand Reinhold: New York, 1992; Chapter 14.

(6) See, for examples: (a) Nesterov, G. A.; Zakharov, V. A.; Fink, G.; Fenzl, W. *J. Mol. Catal.* **1991**, *69*, 129. (b) Collins, S.; Kelly, W. M.; Holden, D. A. *Macromolecules* **1992**, *25*, 1780. (c) Hlatky, G. G.; Upton, D. J. *Macromolecules* **1996**, *29*, 8019.

(7) See, for examples: (a) Bent, B. E.; Nuzzo, R. G.; Dubois, L. H. *J. Am. Chem. Soc.* **1989**, *111*, 1634. (b) Spencer, J. T. *Prog. Inorg. Chem.* **1994**, *41*, 145. (c) Hoffman, D. M. *Polyhedron* **1994**, *13*, 1169.

(8) (a) Kresge, C. T.; Leonowicz, M. E.; Roth, W. J.; Vartuli, J. C.; Beck, J. S. *Nature* **1992**, *359*, 710. (b) Beck, J. S.; Vartuli, J. C.; Roth, W. J.; Leonowicz, M. E.; Kresge, C. T.; Schmitt, K. D.; Chu, C. T.-W.; Olson, D. H.; Sheppard, E. W.; McCullen, S. B.; Higgins, J. B.; Schlenker, J. L. *J. Am. Chem. Soc.* **1992**, *114*, 10834.

(9) Di Renzo, F.; Cambon, H.; Dutartre, R. *Microporous Mater.* **1997**, *10*, 283.

(10) Anwander, R.; Roesky, R. *J. Chem. Soc., Dalton Trans.* **1997**, 137.

(11) See, review article: (a) Schüth, F. *Ber. Bunsenges. Phys. Chem.* **1995**, *99*, 1306. (b) Zakharov, V. A.; Yermakov, Y. I. *Catal. Rev.—Sci. Eng.* **1979**, *19*, 67. (c) Sayari, A. *Stud. Surf. Sci. Catal.* **1996**, *102*, 1. (d) Corma, A. *Chem. Rev.* **1997**, *97*, 2373.

S0276-7333(97)01063-7 CCC: $15.00
Publication on Web 04/21/1998

Scheme 1. Chemisorption of $AlMe_3$ on Silica Surfaces

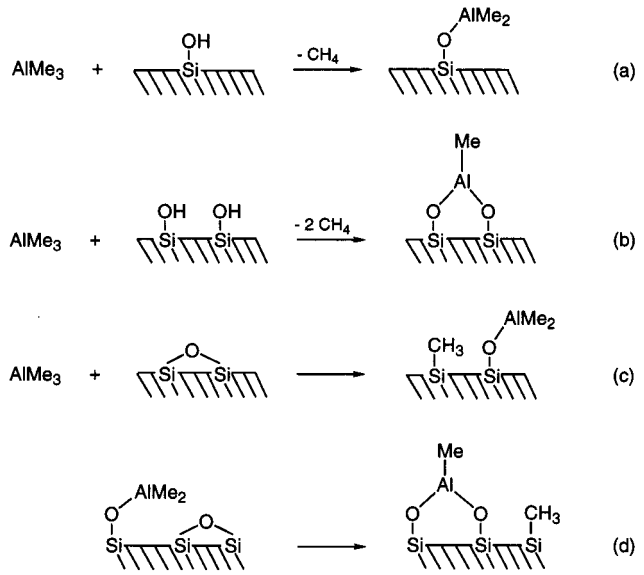

41 host/guest systems derived from main-group[12] and d-transition organometallics[13] have previously been described. We are currently interested in synthesizing supramolecular systems featuring the components MCM-41 and $AlMe_3$ for several reasons. The fundamental question of the extent of the $Si-CH_3$ and $Al-CH_3$ formation originating from a multifunctional reaction of trimethylaluminum on silica surfaces according to Scheme 1 is still under discussion.[14]

The generation of sterically unsaturated, three-coordinate Al species on a well-defined surface results in strongly Lewis acidic centers of composition $(\equiv SiO)_xAlMe_y$ $(x + y = 3)$. Such immobilized aluminum species may widen the scope of similarly composed molecular precatalysts in fine chemical synthesis[15] with regard to separation, recovery, and reuse of the catalyst. In this context, $AlMe_3$-modified "molecular silica surfaces", e.g., alumosilsesquioxanes, provided further insight into both the formation of catalytically active polymeric Lewis acids[16] and the alkylation mode of aluminum alkyl compounds.[17] Finally, the "Ziegler–Natta polymerization" and "methylalumoxane" research[18] is still putting enhanced emphasis on the role of organoaluminum compounds.[19] For example, to trimethylaluminum is ascribed a multifunctional role in the metallocene polymerization process as (i) a scavenger of moisture, while simultaneously compatibilizing, e.g., silica or zeolitic hydroxyl functionalities for the subsequent immobilization of metallocene complexes,[6,20] (ii) a cocatalyst,[19a,21] (iii) an alkylating agent,[19b] and (iv) a component that also mediates chain transfer.[22] In this paper, we present our results on the grafting of trimethylaluminum onto purely siliceous MCM-41, including a detailed solid-state NMR investigation of the resulting supramolecular species. Furthermore, we introduce an efficient reaction for probing the Lewis acidity and alkylation capability of the modified support materials.

Results and Discussion

Stoichiometry of the Chemisorption of $AlMe_3$ on Mesoporous MCM-41. The more detailed examinations of the reaction of $AlMe_3$ with silica materials described so far were performed by contacting the oxidic support with a continuous flow of $AlMe_3$ at reduced pressures.[4,5,14] It was shown that the preannealing temperature of the support, e.g., the degree of dehydration, hardly affects the overall stoichiometry of the chemisorption.[14] In addition, previous investigations revealed that $AlMe_3$ reacts with both isolated and hydrogen-bonded SiOH groups and with strained siloxane bridges, often designated as $(Si-O)_n$ $(n = 2, 3)$. The latter preferably form at increased annealing temperatures. This multifunctional reactivity of aluminum alkyls resulting in the formation of thermodynamically stable Al–siloxide σ bonds was explicitly shown by the corresponding transformations on the molecular level.[23] We have chosen *n*-hexane as an appropriate medium for the chemisorption of $AlMe_3$. The aluminum-free MCM-41 material **1** used in this study was synthesized according to the literature, employing $[C_{16}H_{33}N(CH_3)_3]$-Br as a templating agent.[8,24] After calcination (N_2, 540 °C, 5 h, heating rate 1.5 °C min^{-1}; air, 540 °C, 5 h) and dehydration (10^{-5} Torr, 280 °C, 4 h, heating rate 1 °C min^{-1}), material **1** was characterized by XRD (calcined, $d_{100} = 39.4$ Å), nitrogen adsorption/desorption isotherms (Table 1), and FTIR-spectroscopy (ν(O–H) 3695 cm^{-1}, ν_{as}(Si–OH) 980 cm^{-1}).[25] Treatment of dehydrated MCM-41 (**1**) with $AlMe_3$ is assumed to generate silica-analogous surface species, as depicted in Scheme 2. A typical grafting run involved the addition of an $AlMe_3$/

(12) Huber, C.; Moller, K.; Bein, T. *J. Chem. Soc., Chem. Commun.* **1994**, 2619.
(13) (a) Maschmeyer, T.; Rey, F.; Sankar, G.; Thomas, J. M. *Nature* **1995**, *378*, 159. (b) Ko, Y. S.; Han, T. K.; Park, J. W.; Woo, S. I. *Macromol. Rapid Commun.* **1996**, *17*, 749. (c) Tudor, J.; O'Hare, D. *Chem. Commun.* **1997**, 603. (d) O'Brien, S.; Tudor, J.; Barlow, S.; Drewitt, M. J.; Heyes, S. J.; O'Hare, D. *Chem. Commun.* **1997**, 641.
(14) Bartram, M. E.; Michalske, T. A.; Rogers, J. W., Jr. *J. Phys. Chem.* **1991**, *95*, 4453.
(15) See, for recent examples: (a) Commereuc, D. *J. Chem. Soc., Chem. Commun.* **1995**, 791. (b) Concepcion, A. B.; Maruoka, K.; Yamamoto, H. *Tetrahedron* **1995**, *51*, 4011. (c) Nishiuchi, M.; Honda, K.; Nakai, T. *Chem. Lett.* **1996**, 321. (d) Arai, T.; Sasai, H.; Aoe, K.; Okamura, K.; Date, T.; Shibasaki, M. *Angew. Chem., Int. Ed. Engl.* **1996**, *35*, 104. (e) Gerster, M.; Schenk, K.; Renaud, P. *Angew. Chem., Int. Ed. Engl.* **1996**, *35*, 2396.
(16) Abbenhuis, H. C. L.; van Herwijnen, H. W. G.; van Santen, R. A. *Chem. Commun.* **1996**, 1941.
(17) (a) Feher, F. J.; Blanski, R. L. *J. Am. Chem. Soc.* **1992**, *114*, 5886. (b) Feher, F. J.; Walzer, J. F.; Blanski, R. L. *J. Am. Chem. Soc.* **1991**, *113*, 3618.
(18) *Ziegler Catalysts*; Fink, G., Mühlhaupt, R., Brintzinger, H. H., Eds.; Springer-Verlag: Berlin, 1995. (b) Reddy, S. S.; Sivaram, S. *Prog. Polym. Sci.* **1995**, *20*, 309. (c) Brintzinger, H.-H.; Fischer, D.; Mülhaupt, R.; Rieger, B.; Waymouth, R. *Angew. Chem., Int. Ed. Engl.* **1995**, *34*, 1143.
(19) (a) Resconi, L.; Bossi, S.; Abis, L. *Macromolecules* **1990**, *23*, 4489. (b) Cam, D.; Giannini, U. *Makromol. Chem.* **1992**, *193*, 1049. (c) Reddy, S. S.; Shashidhar, G.; Sivaram, S. *Macromolecules* **1993**, *26*, 1180. (d) Thorn-Csányi, E.; Dehmel, J.; Dahlke, B. *Makromol. Symp.* **1995**, *97*, 91. (e) Tritto, I.; Sacchi, M. C.; Locatelli, P.; Li, S. X. *Macromol. Symp.* **1995**, *89*, 289.
(20) (a) Woo, S. I.; Ko, Y. S.; Han, T. K. *Macromol. Rapid Commun.* **1995**, *16*, 489. (b) Braca, G.; Sbrana, G.; Raspolli-Galletti, A. M.; Altomare, A.; Arribas, G.; Michelotti, M.; Ciardelli, F. *J. Mol. Catal. A* **1996**, *107*, 113. (c) Suzuki, T.; Suga, Y. *Polym. Prepr. (Am. Chem. Soc., Div. Polym. Chem.)* **1997**, 207.
(21) Soga, K.; Shiono, T.; Kim, H. J. *Makromol. Chem.* **1993**, *194*, 3499.
(22) Zambelli, A.; Ammendola, P.; Grassi, A.; Longo, P.; Proto, A. *Macromolecules* **1986**, *19*, 2703.
(23) (a) Jenkner, H. *Z. Naturforsch.* **1959**, *14B*, 133. (b) Mehrotra, R. C.; Rai, A. K. *Polyhedron* **1991**, *10*, 1967. (c) Feher, F. J.; Budzichowski, T. A.; Weller, K. J. *Polyhedron* **1993**, *12*, 591.
(24) Boger, T.; Roesky, R.; Gläser, R.; Ernst, S.; Eigenberger, G.; Weitkamp, J. *Microporous Mater.* **1997**, *8*, 79.

Table 1. Analytical Data, Surface Area, Pore Volume, and Pore Diameter of MCM-41 (Hybrid) Materials

sample (equiv of $AlMe_3$)	elemental analysis: wt % C	elemental analysis: wt % Al	a_s(BET)/m^2 g^{-1} (C)[c]	V_p[d]/cm^3 g^{-1}	$d_{p,max}$[e]/Å
1[a]	–	–	1137 (80)	0.85	27
2a (1)[b]	2.71	2.5	1036 (48)	0.78	26.5
2b (2)[b]	5.32	5.1	943 (35)	0.68	26, 22
2c (3)[b]	7.35	6.9	857 (28)	0.58	25.5, 21
2d (4)[b]	8.74	8.7	788 (23)	0.51	25, 21
2e (5)[b]	10.89	10.6	758 (16)	0.45	20
2f (6)[b]	11.23	10.6	742 (17)	0.44	20
2g (10)[b]	11.33	10.75	749 (16)	0.44	20
3a[b]	11.76	6.9	640 (31)	0.35	18
3b[a]	6.23	7.6	827 (48)	0.55	22
4[a]	5.21	0.2	1057 (31)	0.74	24
7[b]	12.35	7.6	672 (25)	0.31	18.5
8[b]	13.28	9.5	659 (27)	0.31	18
2d (THF)[b]	13.09	7.95	642 (32)	0.36	19
1 (THF)[b,f]	5.58	–	949 (27)	0.63	24
1 ($SiHMe_2$)[a,g]	6.45	–	860 (30)	0.58	21.5

[a] Pretreatment temperature 250 °C, 3 h, 10^{-3} Torr. [b] Pretreatment temperature 25 °C, 3 h, 10^{-3} Torr. [c] Specific BET surface area according to eq 3 (C = BET constant). [d] BJH desorption cumulative pore volume of pores between 15 and 40 Å in diameter. [e] Pore diameter according to the maximum (maxima) of the pore size distribution calculated from the desorption branch; d_p < 20 Å resulting from the BJH method have to be viewed critically. [f] Product obtained by suspending material **1** in THF. [g] Product obtained by silylation of material **1** with $HN(SiHMe_2)_2$.[10]

Scheme 2. Possible Surface Species of the Immobilization of $AlMe_3$ on MCM-41 (1)[a]

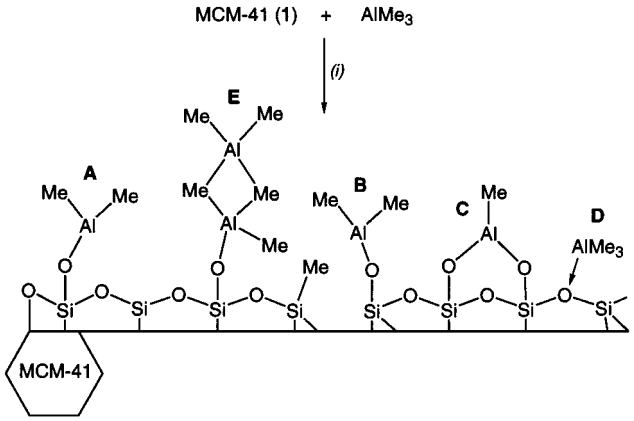

[a] *Conditions*: (*i*) *n*-hexane, ambient temperature, 20 h, 5 h evacuation at 10^{-2} Torr.

n-hexane solution to material **1**, suspended in *n*-hexane, within a period of less than 2 min at ambient temperature. To determine the amount of $AlMe_3$ that is necessary to react with all of the terminal surface hydroxyl groups, the reaction was performed with different molar ratios of $AlMe_3$:**1** (Table 1). The evolution of methane is instantaneous and visibly stops after complete addition of $AlMe_3$. Upon stirring for 20 h, several *n*-hexane washings, and drying under vacuum for 5 h, white powders designated as **2** were obtained.

The hybrid materials **2** do not inflame spontaneously when exposed to air like pure $AlMe_3$ does. However, they change in color to dark brown and react violently with moist solvents. The characterization of materials **2** was performed by means of elemental analysis, FTIR spectroscopy, nitrogen adsorption/desorption isotherms, MAS NMR spectroscopy, and surface reactions (Table 1). In previous studies, FTIR spectroscopy has been extensively applied to characterize $AlMe_3$-chemisorptions on silica.[4,5,14,26] Examination of materials **2** revealed that consumption of all of the active surface sites (Si−OH at 3695 cm^{-1}; SiO at 980 cm^{-1}) is achieved after the addition of 4−5 mmol of $AlMe_3$ per gram of material **1**. Carbon and aluminum elemental analysis of **2a**−**g** tentatively confirmed these findings (Table 1). The data obtained for **2e**−**g**, i.e., as a result of the reaction of **1** with an excess of $AlMe_3$, suggest that additional $AlMe_3$ (<1 equiv) is retained on the surface. This might be due to a slower chemisorption at high surface coverage or due to physisorbed $AlMe_3$ (species **D**, Scheme 2). An accompanying physisorption of $AlMe_3$ on silica support materials has been discussed previously.[27] Considering the BET surface area of approximately 1140 m^2 g^{-1} and the results from elemental analysis, surface saturation of **2e** is achieved at loadings of 2.1 Al/100 $Å^2$ and 4.8 CH_3/100 $Å^2$ (4.0 mmol of Al and 9.1 mmol of CH_3 per gram of **2e**). Previous examinations and models based on $AlMe_3$/silica suggest values of 2.8−3.2 Al/100 $Å^2$ and a maximum methyl population of 8.4/100 $Å^2$.[14] About 25% of the anchored aluminum of **2e** can be degrafted by reaction with excess $HOC(CF_3)_3$ as an alkoxide complex[28] to yield hybrid material **3**. Repeated treatment of sample **2e** with acetylacetone in an ethanolic suspension at 80 °C afforded material **4** and $Al(acac)_3$, originating from extraction of surface aluminum.[29] However, material **4** still contains some aluminum, pointing toward aluminum which has been entirely incorporated into the support (vide infra).

Nitrogen Physisorption Measurements at 77.4 K. The determination of nitrogen adsorption/desorption isotherms is an efficient tool to characterize the nature of porous host systems. Mesoporous materials of type MCM-41 (**1**) display type-IV isotherms according to IUPAC nomenclature,[30] which are characterized by a sharp inflection point due to capillary condensation (Figure 1a). This part of the isotherm is consulted to derive the pore size distribution and the effective mesopore diameter on the basis of the Kelvin equation (Figure 1b, Experimental Section). The effective mean pore diameter of material **1** is obtained as 26 Å. Exposure of material **1** to different quantities of $AlMe_3$ resulted in N_2 adsorption/desorption isotherms that show the gradual filling of the mesopores (Figure 1, **2a**−**f**). The BJH differential pore size distribution obtained for **2a**−**d**, i.e., at incomplete $AlMe_3$ loading, displays two

(25) See, for IR spectroscopic characterization of MCM-41 materials: (a) Chen, J.; Li, Q.; Xu, R.; Xiao, F. *Angew. Chem., Int. Ed. Engl.* **1995**, *34*, 2898. (b) Ishikawa, T.; Matsuda, M.; Yasukawa, A.; Kandori, K.; Inagaki, S.; Fukushima, T.; Kondo, S. *J. Chem. Soc., Faraday Trans.* **1996**, *92*, 1985. (c) Jentys, A.; Pham, N. H.; Vinek, H. *J. Chem. Soc., Faraday Trans.* **1996**, *92*, 3287.

(26) (a) Yates, D. J. C.; Dembinski, G. W.; Kroll, W. R.; Elliott, J. J. *J. Phys. Chem.* **1969**, *73*, 911. (b) Low, M. J. D.; Severdia, A. G.; Chan, J. *J. Catal.* **1981**, *69*, 384. (c) Dodonova, V. A.; Molotovshchikova, M. B.; Titov, V. A.; Sedova, L. G.; Postinkova, T. K. *Organomet. Chem. USSR* **1991**, *4*, 544. (d) Kinney, J. B.; Staley, R. H. *J. Phys. Chem.* **1983**, *87*, 3735.

(27) Ciardelli, F.; Altomare, A.; Conti, G.; Arribas, G.; Mendez, B.; Ismayel, A.; *Macromol. Symp.* **1994**, *80*, 29.

(28) Willis, J. C. *Coord. Chem. Rev.* **1988**, *88*, 133.

(29) Bosacek, V.; Freude, D.; Fröhlich, T.; Pfeifer, H.; Schmiedel, H. *J. Colloid Interface Sci.* **1982**, *85*, 502.

(30) Sing, K. S. W.; Everett, D. H.; Haul, R. A. W.; Moscou, L.; Pierotti, R. A.; Rouquérol, J.; Siemieniewska, T. *Pure Appl. Chem.* **1985**, *57*, 603.

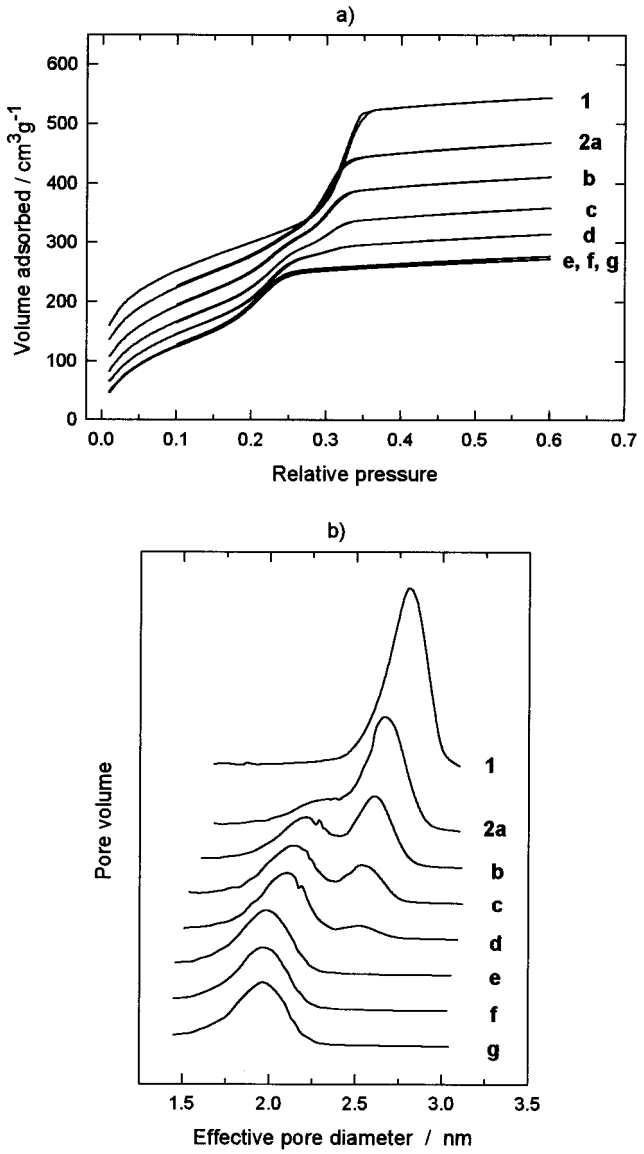

Figure 1. (a) Nitrogen adsorption/desorption isotherms at 77.4 K of untreated, activated MCM-41 (**1**) and after reaction with various amounts of $AlMe_3$ (**2a**−**g** according to Table 1); (b) BJH differential pore size distribution obtained from the isotherms of a.

well-resolved pore size maxima at approximately 20 and 26 Å. This fact can only be ascribed to the presence of two different pore systems, that is, apparently unloaded pores and $AlMe_3$-loaded pores. Clearly, this type of mesopore filling hints at the rate-determining step of the immobilization reaction, and this will be discussed below in more detail. The maximum surface population produces materials **2e**−**g**, where all of the original large mesopores are transformed into smaller ones. The $AlMe_3$-saturated materials still display type-IV isotherms. The details of the isotherms resemble those found in a $HN(SiHMe_2)_2$-silylated MCM-41 material, which contains "$OSiHMe_2$" surface species with a similar steric requirement (Table 1).[10] However, the pore volume of **2e**−**g** is significantly smaller compared to that of the silylated material. This is plausible considering the multifunctional reaction of $AlMe_3$ compared to the monofunctional reaction of the bulkier $HN(SiHMe_2)_2$ agent. Furthermore, the nitrogen physisorption measurements are in accord with the results from elemental

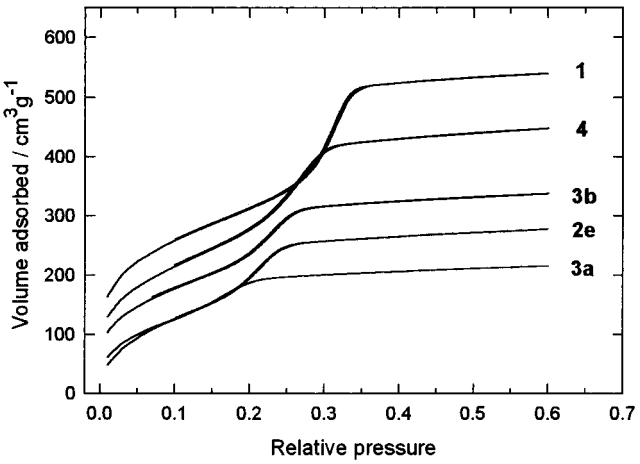

Figure 2. Nitrogen adsorption/desorption isotherms at 77.4 K of untreated, activated MCM-41 (**1**) and **2e** treated with $HOC(CF_3)_3$ (**3a**,**b**) and Hacac (**4**) (compare to Table 1).

analysis, indicating surface saturation at increasing $AlMe_3$ loadings.

Figure 2 shows the nitrogen adsorption/desorption isotherms of the materials obtained from the extraction experiments of **2e** with $HOC(CF_3)_3$ and acetylacetone, respectively. Treatment of **2e** with the perfluorinated alcohol provides a material **3a**, which after the usual workup procedure still contains a considerable amount of physisorbed molecular components, such as alkoxide complexes. Part of these species are desorbed upon thermal treatment at 250 °C/10^{-2} Torr for 3 h to yield material **3b**. This is indicated by an increased pore volume of **3b** (Table 1). Material **4**, which was obtained by the acetylacetone/ethanol treatment, exhibits an effective pore diameter of 24 Å, between that of **1** and **2e**. This can be explained by the presence of pore size limiting, nonextractable $Si-CH_3$ groups (Figure 2).

Solid-State NMR Characterization. MAS NMR spectroscopy has proven to be a useful method to monitor surface reactions of organometallic reagents.[31] However, to the best of our knowledge, there are no detailed MAS NMR studies on $AlMe_3$-modified silica materials. The ^{1}H MAS NMR spectrum of dehydrated siliceous MCM-41 (**1**) is shown in Figure 3A. The peak maximum, located at 1.8 ppm, is attributed to isolated ≡Si−OH groups by comparison with the results obtained for dehydrated mesoporous and conventional silica materials.[32]

In the following, we thoroughly examined sample **2d** (4 equiv reaction, Table 1) which, according to the FTIR spectrum, contains a small quantity of unreacted hydroxyl groups. It can be assumed that this material contains no or only a very small amount of physisorbed $AlMe_3$. The ^{1}H MAS NMR spectrum of **2d** shows a broad resonance centered at 0.2 ppm exhibiting two well-resolved shoulders (Figure 3B). The simulation of the spectrum reveals three component lines located at 1.7, 0.2, and −0.7 ppm with relative signal intensities of approximately 2%, 30%, and 68%, respectively (Figure

(31) Reven, L. *J. Mol. Catal.* **1994**, *86*, 447.
(32) (a) Haukka, S.; Lakomaa, E.-L.; Root, A. *J. Phys. Chem.* **1993**, *97*, 5085. (b) Haukka, S.; Root, A. *J. Phys. Chem.* **1994**, *98*, 1695 and references therein. (c) Turov, V. V.; Leboda, R.; Bogillo, V. I.; Skubiszewska-Zieba, J. *Langmuir* **1997**, *13*, 1237.

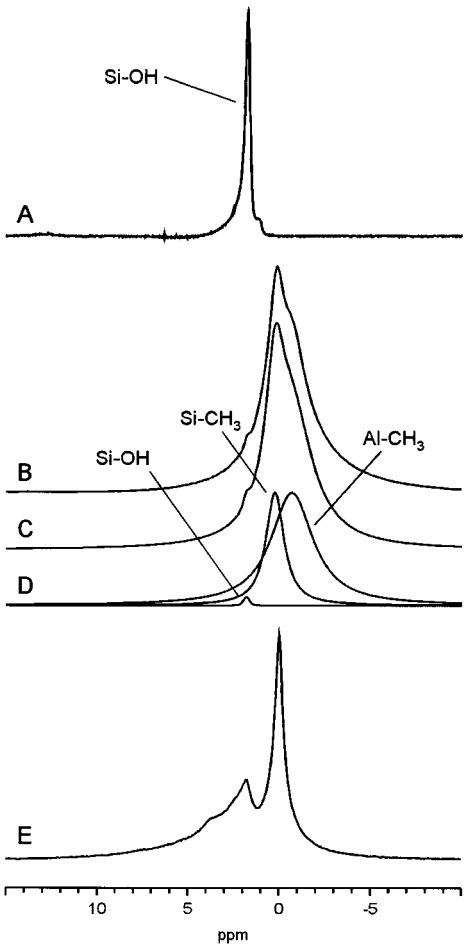

Figure 3. ^{1}H MAS NMR spectra of sample **1** and **2d**: (A) **1** dehydrated at 280 °C/10^{-4} Torr; (B) **2d** washed several times with *n*-hexane, evacuated for 5 h at 25 °C/10^{-2} Torr; (C) simulated spectrum; (D) components of simulation; (E) **2d** exposed to air for 14 days (completely hydrolyzed) and dehydrated for 12 h at 200 °C/10^{-2} Torr.

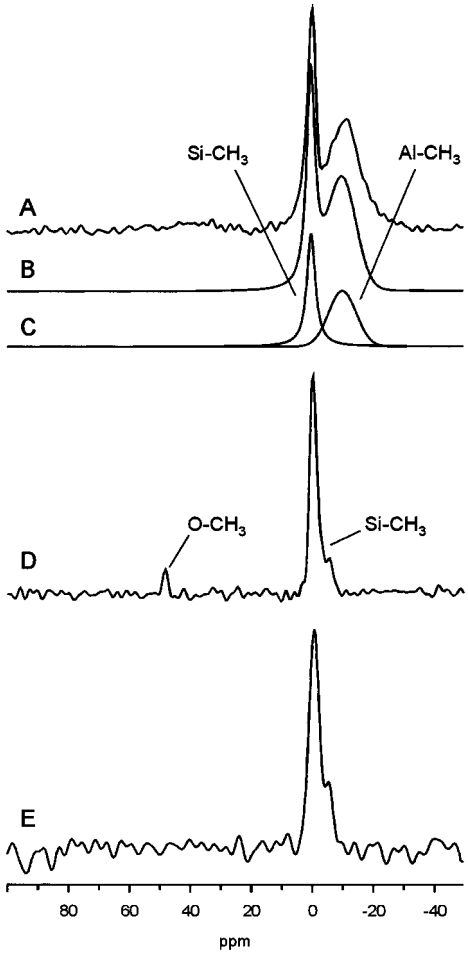

Figure 4. ^{13}C MAS NMR spectra of sample **2d**: (A) washed several times with *n*-hexane and evacuated for 5 h at 25 °C/10^{-2} Torr; (B) simulated spectrum; (C) components of simulation; (D) exposed to air for 2 days; (E) exposed to air for 14 days (completely hydrolyzed) and dehydrated for 12 h at 200 °C/10^{-2} Torr.

3C,D). The chemical shifts can be assigned to three physically significant species at the surface. The signal at 1.7 ppm reflects the small amount of residual silanol groups by comparison with Figure 3A. The resonance at 0.2 ppm is attributable to ≡Si−CH_3 groups. Finally, the peak centered at −0.7 ppm can be assigned to Al−CH_3 surface moieties. The broadening of the latter signal is probably due to the coexistence of different Al−CH_3 surface species, including (≡SiO)$AlMe_2$ and (≡SiO)$_2$-AlMe with different coordination geometries at the aluminum center. For comparison, the ^{1}H signals of aluminum methyl ligands are reported at −0.43 ppm for $MeAl(OC_6H_2tBu_2$-2,6-Me-4)$_2$ and −0.20 ppm for Me_2-$Al(OC_6H_2tBu_2$-2,6-Me-4).[33] Air-exposure of sample **2d** results in the complete disappearance of the signal at −0.7 ppm, whereas the peak of the nonhydrolyzable silicon methyls is retained (Figure 3E). In addition, a broad resonance ranging from about 1 to about 8.0 ppm appears, which is attributed to the Si−OH and Al−OH groups partly involved in hydrogen bonds.[34] The ^{1}H MAS NMR spectra of $AlMe_3$-saturated samples **2e**−**g** (not shown) exhibit only two resonances at 0.2 ppm due to ≡Si−CH_3 (relative intensity 29%) and at −0.6 ppm due to Al−CH_3 (71%), which reveals the complete consumption of all of the hydroxyl functionalities.

The ^{13}C CPMAS NMR spectra of sample **2d** are presented in Figure 4. Two peaks were detected which could be successfully decomposed into a narrower Lorentzian (340 Hz width) and a broad Gaussian line shape (1100 Hz width) (Figure 4A−C). The narrower peak at 0.1 ppm is straightforwardly attributable to ≡Si−CH_3 groups.[35] The broad peak observed at −9.5 ppm can be assigned to Al−CH_3 moieties. The signal broadening of the latter ^{13}C resonance probably arises not only from differently composed Al−CH_3 surface species (vide supra) but might also be principally affected by quadrupolar interactions with the directly attached aluminum (^{27}Al, $I = {}^{5}/_{2}$).[36] The relative intensities of 32% and 68% are in accord with the findings from the ^{1}H MAS NMR study. Similar shifts of surface-bonded Al−CH_3 groups have been reported previously in the case of, e.g., the immobilization of

(33) (a) Shreve, A. P.; Mülhaupt, R.; Fultz, W.; Calabrese, J.; Robbins, W.; Ittel, S. D. *Organometallics* **1988**, *7*, 409. (b) Healy, M. D.; Wierda, D. A.; Barron, A. R. *Organometallics* **1988**, *7*, 2543.

(34) See, for example: Fitzgerald, J. J.; Piedra, G.; Dec, S. F.; Seger, M.; Maciel, G. E. *J. Am. Chem. Soc.* **1997**, *119*, 7832.

(35) Toscano, P. J.; Marks, T. J. *J. Am. Chem. Soc.* **1985**, *107*, 653.

(36) Turunen, J.; Pakkanen, T. T.; Löfgren, B. *J. Mol. Catal. A* **1997**, *123*, 35.

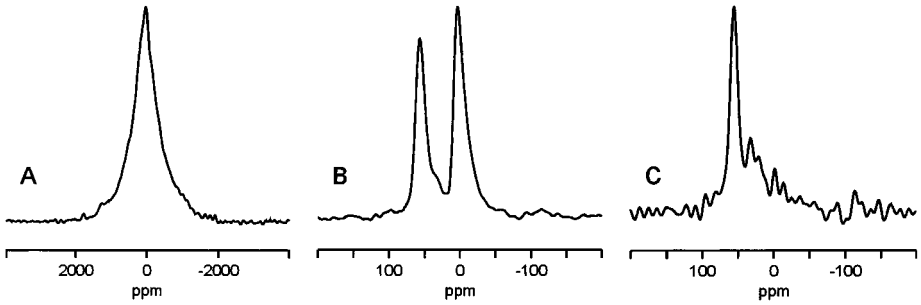

Figure 5. ^{27}Al NMR spectra of sample **2d** and **2e**: (A) **2d** washed several times with *n*-hexane, evacuated for 5 h at 25 °C/10^{-2} Torr; (B) **2d** exposed to air for 14 days (completely hydrolyzed); (C) **2e** extracted several times with an ethanolic solution of Hacac at 80 °C and washed several times with THF.

$Cp^*_2Th(^{13}CH_3)_2$ on dehydroxylated alumina (−12 ppm)[35] or treatment of partially hydrated silica with $AlMe_3$ (−7.7 ppm).[37] ^{13}C NMR solution spectra of $AlMe_3$ (−7.1 ppm, in toluene),[38] $AlMe_3$(THF) (−8.6 to −9.0 ppm, in toluene),[38] $MeAl(OC_6H_2tBu_2\text{-}2,6\text{-}Me\text{-}4)_2$ (−9.1 ppm, in toluene),[39] and $Me_2Al[OC_6H_4(CH_2NMe_2)\text{-}2]\cdot xAlMe_3$ (−5.10 ppm ($AlMe_3$); −9.67 ppm ($AlMe_2$), in benzene)[40] may be also consulted for comparison. Interestingly, a similarly shaped signal is observed for methylalumoxane (−6.6 to −7.8 ppm).[41] As expected, the signal of the Al−CH_3 groups in **2d** disappeared upon air-exposure (Figure 4D,E). A possible degradation product could be trapped according to spectrum D of Figure 4, exhibiting a clearly visible resonance at approximately 60 ppm attributable to an OCH_3 moiety. The final spectrum E of Figure 4 supports hydrolysis of a methoxide intermediate and subsequent slow desorption of methanol. The formation of surface-bonded alkoxide species via partial oxidation of metal−carbon bonds has been mentioned earlier[41b,42] and was examined thoroughly in the solution chemistry.[43]

We also attempted to characterize the aluminum sites of sample **2d** by ^{27}Al MAS NMR.[44] However, no signal could be obtained in the MAS NMR spectrum, even at fast (10 kHz) MAS spinning rates and large numbers of spectra accumulations. Considering the high aluminum content of the sample, this result is probably due to a distribution of surface-docked alumoxo−alkyl sites in highly distorted coordination environments. This gives rise to very strong quadrupolar interactions, rendering the ^{27}Al resonance unobservable under MAS conditions.[45] However, as shown in Figure 5A, a strong and very broad resonance appears in the ^{27}Al NMR spectrum of sample **2d** measured under static conditions (i.e., without MAS), applying a quadrupole echo pulse sequence. The presence of "MAS NMR invisible" aluminum has been concluded previously from strongly distorted AlO_4 environments in dehydrated zeolites.[46] It also was shown that this part could be made visible by application of static ^{27}Al NMR experiments. The broad line shape of the signal of Figure 5A documents the large quadrupolar interaction of the aluminum sites and may be further affected by the coexistence of aluminum in different coordination environments. Neglecting the latter effect, a quadrupole coupling constant (e^2qQ/h) of about 15 MHz could be estimated from the line width. After hydrolysis of all of the Al−CH_3 groups by exposing sample **2d** to humid air, the coordination symmetry of the aluminum sites is relaxed. The resulting ^{27}Al MAS NMR spectrum now features two well-resolved resonances at 56 and 4 ppm (Figure 5B), indicative of 4- and 6-fold oxygen-coordinated aluminum.[47] The weak shoulder at about 35 ppm points to the presence of small amounts (<10%) of five-coordinate Al.

Repeated extraction of **2e** with the chelating agent acetylacetone removes most of the aluminum from the pores (Figure 5C).[29] However, abstraction of the four- and five-coordinate Al seems to be hindered. The chemical shift of 55 ppm of the remaining largest signal is typical of an $Al(OSi)_4$ environment in framework aluminosilicates. Consequently, treatment of dehydrated MCM-41 with $AlMe_3$ and subsequent slow hydrolysis result in the incorporation of tetrahedral aluminum into the surface of silica walls. Better control of both the postsynthesis incorporation of aluminum in structurally highly ordered all-silica MCM-41 and the subsequent extraction procedures might, thus, present an attractive alternative to the conventional preparation of aluminosilicate MCM-41 by hydrothermal synthesis.[48] According to the latter standard procedures, higher Al content (Si/Al < 10) usually results in extensive formation of six-coordinate nonframework aluminum.[49] In addition, the former method involves the incorporation of tetrahedral aluminum at or near

(37) Lee, D.-H.; Shin, S.-Y.; Lee, D. H. *Macromol Symp.* **1995**, *97*, 195.
(38) (a) Anwander, R.; Runte, O.; Eppinger, J.; Gerstberger, G.; Herdtweck, E.; Spiegler, M. *J. Chem. Soc., Dalton Trans.* **1998**, 847. (b) Byers, J. J.; Pennington, W. T.; Robinson, G. H.; Hrncir, D. C. *Polyhedron* **1990**, *9*, 2205.
(39) Benn, R.; Janssen, E.; Lehmkuhl, H.; Rufinska, A.; Angermund, K.; Metz, P.; Goddard, R.; Krüger, C. *J. Organomet. Chem.* **1991**, *411*, 37.
(40) Hogerheide, M. P.; Wesseling, M.; Jastrzebski, J. T. B. H.; Boersma, J.; Kooijman, H.; Spek, A. L.; van Koten, G. *Organometallics* **1995**, *14*, 4483.
(41) (a) Giannetti, E.; Nicoletti, G. M.; Mazzocchi, R. *J. Polym. Sci.* **1985**, *23*, 2117. (b) Janiak, C.; Rieger, B.; Voelkel, R.; Braun, H.-G. *J. Polym. Sci.* **1993**, *31*, 2959.
(42) Quignard, F.; Lecuyer, C.; Bougault, C.; Lefebvre, F.; Choplin, A.; Olivier, D.; Basset, J.-M. *Inorg. Chem.* **1992**, *31*, 928.
(43) (a) Barron, A. R. *Chem. Soc. Rev.* **1993**, 93. (b) Lewinski, J.; Zachara, J.; Grabska, E. *J. Am. Chem. Soc.* **1996**, *118*, 6794.
(44) (a) Fyfe, C. A.; Thomas, J. M.; Klinowski, J.; Gobbi, G. C. *Angew. Chem., Int. Ed. Engl.* **1983**, *22*, 259. (b) Klinowski, J. *Chem. Rev.* **1991**, *91*, 1459.
(45) Potapov, A. G.; Terskikh, V. V.; Bukatov, G. D.; Zakharov, V. A. *J. Mol. Catal. A* **1997**, *122*, 61.
(46) Freude, D.; Ernst, H.; Wolf, I. *Solid State Nucl. Magn. Reson.* **1994**, *3*, 2713.
(47) Engelhardt, G.; Michel, D. *High-resolution solid-state NMR of silicates and zeolites*; Wiley: New York, 1987.
(48) See, for example: Chen, C.-Y.; Li, H.-X.; Davis, M. E. *Microporous Mater.* **1993**, *2*, 17.
(49) See, for examples: (a) Kloestra, K. R.; Zandbergen, H. W.; van Bekkum, H. *Catal. Lett.* **1995**, *31*, 157. (b) Luan, Z.; Cheng, C.-F.; Zhou, W.; Klinowski, J. *J. Phys. Chem.* **1995**, *99*, 1018. (c) Borade, R. B.; Clearfield, A. *Catal. Lett.* **1995**, *31*, 267.

Scheme 3. Pore-Filling Models for the Reaction of 1 with $AlMe_3$ at Incomplete Loading

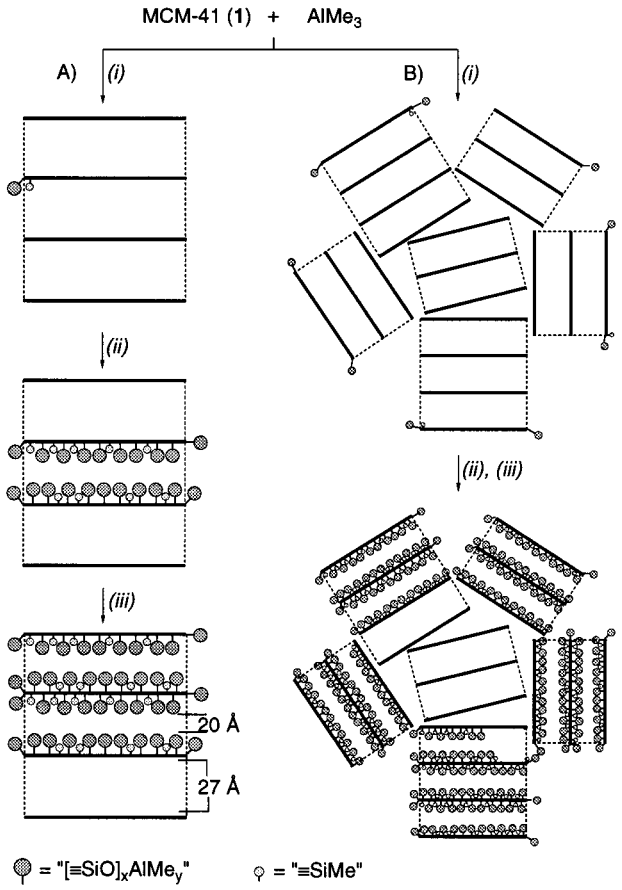

to the pore surface, which may be of particular interest in the application of these materials in acid catalysis.[11]

Mechanism of Chemisorption. Given the results of the elemental analysis, N_2 physisorption measurements, and solid-state NMR spectroscopy, we are tempted to suggest a mechanistic scenario for the immobilization reaction. The appearance of two well-separated maxima in the calculated pore size distribution of $AlMe_3$-unsaturated materials **2a**−**d** (Figure 1b) implies the presence of unmodified pores of about 26 Å diameter and of confined $AlMe_3$-modified pores with an effective diameter of about 20 Å. This means that the filling of a portion of pores seems to be finished when the loading of others has not yet started.

Assuming that in a highly dispersed powder suspension of **1** with primary particles in the nanosize regime all mesopores are equally accessible to the organometallic agent, the following initial steps of chemisorption are proposed (Scheme 3, A): (i) the diffusion of trimethylaluminum into the pores and onto the surface of the support is slow compared to the surface reaction; (ii) the initially immobilized species might direct the hydrophobicity of the surface in such a way that approaching trimethylaluminum molecules are guided preferentially into the same pore; (iii) adjacent pores are filled analogously.

We favor an alternative pore-filling procedure, as depicted in Scheme 3, B. This model is based on the assumption that sufficiently large agglomerates of silicate MCM-41 are present in the starting *n*-hexane suspension, i.e., nanosized uniform mesopore arrays are stuck together in the form of microsized particles,[50] and (i) each trimethylaluminum rapidly reacts with the nearest support surface site; (ii) the chemisorption proceeds regularly from the outer areas to the interior of the MCM-41 agglomerate; and (iii) the filling of the uniform mesopore arrays may involve the steps as proposed in model A.

The $AlMe_3$/silica reaction was shown to be nonselective with respect to the different surface sites represented by isolated and hydrogen-bonded hydroxyl and strained siloxane bridges.[14] On the basis of FTIR and X-ray photoelectron spectroscopy, a model, involving surface species **A**−**D** (Scheme 2) was suggested. According to this model, C/Al atomic ratios as high as 2.8 (XPS) and monomethylaluminum as well as monomethylsilicon groups as the major species on the surface, averaging at 14/100 Å^2, were predicted.[14] Our calculations from elemental analysis of **2e** give a C/Al atomic ratio of 2.3 and aluminum and methyl populations of 2.1/100 Å^2 and 4.8/100 Å^2, respectively, on a saturated, curved surface. In addition, analysis of the ^{1}H and ^{13}C MAS NMR studies favors Si−CH_3/Al−CH_3 ratios as low as approximately 0.45. Hence, the relatively high Al−CH_3 population may suggest the presence of a considerable amount of dimethylaluminum groups on the surface. Furthermore, we would like to consider additional organoaluminum species **D** and **E**. $AlMe_3$-oversaturated surface areas might produce **E**-type species which formally result from the addition of physisorbed $AlMe_3$ (**D**) to surface species **A** and **B**. The corresponding addition reactions have been demonstrated in soluble monoalkylaluminum aryloxide complexes.[33] The formation of **E**-type species does not contradict the findings obtained by nitrogen physisorption measurements**.** The presence of different organoaluminum surface species in **2** also seems to be plausible from the spectroscopic investigation of air-exposed samples of **2d**. At least two major aluminum sites are formed according to the ^{27}Al MAS NMR spectrum shown in Figure 5B. The ^{27}Al NMR spectrum of **2d** obtained under static conditions further suggests the presence of aluminum centers exhibiting a highly polarized charge density corresponding to a distorted coordination geometry. Such aluminum species may emerge from the docking of $AlMe_3$ at sterically rigid, electron-deficient surface sites and can be considered as destabilized in terms of enhanced reactivity.[17]

Rare Earth Dimethylsilyl Amides—Probes for the Desolvation and Alkylation Capability of $AlMe_3$-Modified MCM-41 (2). Formally "three-coordinated", geometrically distorted surface species of the type $(\equiv SiO)_xAlMe_y$ ($x + y = 3$), prevented from self-association by surface confinement, should display considerable Lewis acidity.[51] A simple way to characterize the Lewis acidic strength can be accomplished by intermetallic Lewis acid-base competition reactions, as previously shown in homogeneous systems.[52] Very recently, we found that $AlMe_3$ can displace one THF ligand at the less Lewis acidic yttrium center in

(50) Grün, M.; Lauer, I.; Unger, K. K. *Adv. Mater.* **1997**, *9*, 254.
(51) (a) Power, M. B.; Nash, J. R.; Healy, M. D.; Barron, A. R. *Organometallics* **1992**, *11*, 1830. (b) Barron, A. R. *Polyhedron* **1995**, *14*, 3197.
(52) Stults, S. D.; Andersen, R. A.; Zalkin, A. *Organometallics* **1990**, *9*, 115.

$Y[N(SiHMe_2)_2]_3(THF)_2$ (**5**) according to eq 1.[38] The

$$\underset{\mathbf{5}}{Y[N(SiHMe_2)_2]_3(THF)_2} + AlMe_3 \rightarrow \underset{\mathbf{6}}{Y[N(SiHMe_2)_2]_3(THF)} + AlMe_3(THF) \quad (1)$$

resulting mono(THF) adduct **6** can be easily distinguished from **5** due to the peculiar spectroscopic characteristics of the SiH moiety.

Separation of $Y[N(SiHMe_2)_2]_3(THF)$ (**6**) and $AlMe_3$-(THF) is hampered by both their high solubility in aliphatic hydrocarbons and their low tendency of crystallization. The feasibility of a heterogeneously performed transformation corresponding to eq 1 employing hybrid material **2** as a suitably modified, solid Lewis acid might eliminate such separation problems. In additon, lanthanide dialkylamide complexes[53] and also the system $Y[N(SiHMe_2)_2]_3(THF)_2$ (**5**)[38] are prone to alkylation in the presence of excess $AlMe_3$ (eq 2).

$$\underset{\mathbf{5}}{Y[N(SiHMe_2)_2]_3(THF)_2} + \text{excess } AlMe_3 \rightarrow \underset{\mathbf{9}}{Y[(\mu\text{-}Me)_2AlMe_2]_3} + \underset{\mathbf{10}}{\{Me_2Al[\mu\text{-}N(SiHMe_2)_2\}_2} + AlMe_3(THF) + \text{unsoluble product} \quad (2)$$

Transfer of an optional alkylation to a heterogeneous system would be desirable in terms of evaluating the alkylating capability of support materials such as **2**.

The aluminated hybrid material **2d** was initially employed to exclude ("minimize") the presence of physisorbed $AlMe_3$ along with its potential alkylating effect. A solution of **5** in *n*-hexane was added to a suspension of an *excess* of **2d** in *n*-hexane. Several *n*-hexane washings and drying of the residue afforded a white material **7**. An FTIR spectroscopic study of **7** revealed the consumption of the residual surface hydroxyl groups via a siloxide formation/silylation reaction pathway (ν(SiH) = 2151, 2085 cm^{-1}).[10] Elemental analysis and spectroscopic examinations of the residue of the combined *n*-hexane fractions are consistent with the displacement of one THF ligand in **5** and the formation of $Y[N(SiHMe_2)_2]_3(THF)$ (**6**) according to Scheme 4. The IR spectrum of **6** exhibits two well-separated SiH stretching vibrations at 2067 and 1931 cm^{-1}, the latter being indicative of a pronounced β-SiH···Y interaction.[38] The ^1H NMR signal of the SiH proton is shifted downfield to 4.92 ppm compared to the starting material **5** (4.99 ppm, $^1J_{SiH}$ = 171 Hz) and exhibits a decreased $^1J_{SiH}$ coupling of 161 Hz. N_2 physisorption measurements of **7** show the complete consumption of mesopores centered at 26 Å, indicating that these pores are readily accessible to the bulkier yttrium amide complexes. The mesopores originally displaying an effective mean diameter of 20 Å now have one of approximately 18 Å, probably due to the presence of aluminum-bonded THF. A possible interaction of the bulky yttrium amide complex with the surface-bonded aluminum species seems to be negligible on the basis of the adsorption data and the detection of complex **6** in solution. To show the effect of physisorbed THF on the pore characteristics,

(53) Evans, W. J.; Anwander, R.; Doedens, R. J.; Ziller, J. W. *Angew. Chem., Int. Ed. Engl.* **1994**, *33*, 1641.

Scheme 4. Desolvation of $Y[N(SiHMe_2)_2]_3(THF)_2$ (5) over Sample 2d

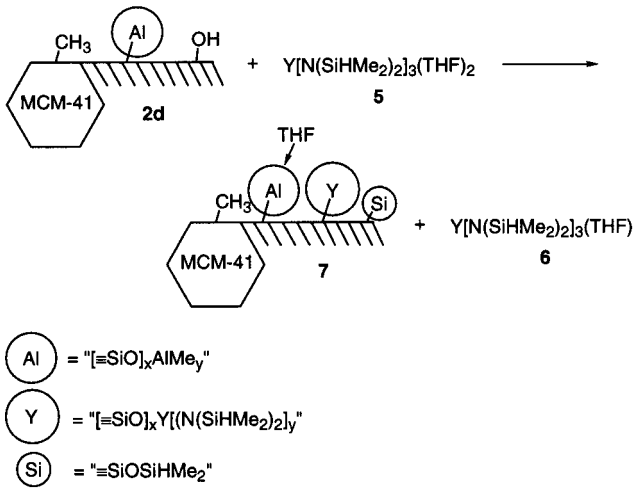

Scheme 5. Desolvation and Alkylation of $Y[N(SiHMe_2)_2]_3(THF)_2$ (5) over Sample 2e

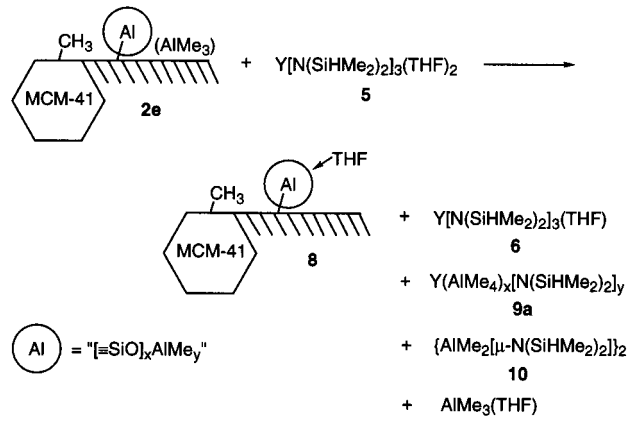

samples of **1** and **2d** were treated with an excess of THF. The physisorption of THF, in the case of **2d** most likely due to adduct formation at surface aluminum centers, reduces the pore volume about 30% (Table 1).

Finally, compound $Y[N(SiHMe_2)_2]_3(THF)_2$ (**5**) was added to a sample of completely aluminated material **2e** which contains no residual hydroxyl groups but some physisorbed $AlMe_3$. The IR spectrum of the resulting hybrid material **8** displays no band in the SiH region assignable to a silylation product. However, weak SiH stretching vibrations at 2182 (Al) and 2088 cm^{-1} (Y) indicate the presence of a considerable amount of metal amide species on the support, as confirmed by ICP analysis (Y, 1.4 wt %). N_2 physisorption measurements reveal that the original pore size of 20 Å (**2e**) is only decreased by 3 Å, probably due to a dominating complexation of THF at the aluminum sites. Correspondingly, the pore volume of **8** is decreased by approximately 30%. Spectroscopic examination of the combined *n*-hexane fractions proved that in addition to the formation of **6** a considerable amount of typical alkylation products can be detected: species **9a**, containing the $Y(AlMe_4)$ moiety and $\{AlMe_2[\mu\text{-}N(SiHMe_2)_2]\}_2$ (**10**),[38b] apparently being formed according to Scheme 5. Spectroscopic details of the alkylation products are described in the Experimental Section.

Conclusion

$AlMe_3$-modified mesoporous silicates can be readily synthesized via solution impregnation of the support material with the organoaluminum reagent in *n*-hexane. N_2 physisorption measurements provide important details of the chemisorption process, including the stepwise filling of the mesopores, indication of surface saturation, and the stability of the mesopore structure toward structural collapse under such hazardous conditions. Characterization of the hybrid materials by elemental analysis, spectroscopy (FTIR, MAS NMR), and surface reactions revealed important features, such as $SiCH_3/AlCH_3$ population ratios of approximately 0.45. Air-exposure and extraction experiments with acetylacetone of the air- and moisture-sensitive hybrid materials indicate the presence of at least two different aluminum species, including the presence of an almost nonextractable component. The remarkable incorporation of aluminum into the silicate surface might have implications for the synthesis of catalytically active mesoporous aluminosilicates. Furthermore, the strong Lewis acidic behavior of the $AlMe_3$-modified material is verified by an intermetallic Lewis acid−base competition reaction involving the spectroscopically versatile *n*-hexane soluble complex $Y[N(SiHMe_2)_2]_3(THF)_2$. One THF base ligand is exchanged and irreversibly bonded to the support under the prevailing conditions. Additionally, we have shown that the rare earth bis(dimethylsilyl)amide is a sensitive agent to probe the alkylation capability of such an organoaluminum-modified support material. We are currently examining the application of this novel "alkylation test reaction" to other $AlMe_3$-containing (contaminated) materials such as methylalumoxane (MAO) in order to determine the accessibility and amount of physisorbed or included $AlMe_3$. The enhanced Lewis acidity of materials **2**, reflected in their increased reactivity toward neutral base ligands, as shown in the case of THF, opens up other possible applications such as complexation chromatography of heteroatom-containing natural products.[54]

Experimental Section

General. The synthesis and manipulation of all compounds and hybrid materials were performed with rigorous exclusion of air and water, using high-vacuum and glovebox techniques (MB Braun MB150B−G-II; <1 ppm of O_2, <1 ppm of H_2O). Solvents were distilled from Na/K alloy (benzophenone ketyl) under nitrogen. $AlMe_3$ and acetylacetone were used as received from Aldrich. $HOC(CF_3)_3$ (Aldrich) was vacuum-distilled before use. $Y[N(SiHMe_2)_2]_3(THF)_2$ was prepared according to the literature.[55] MCM-41 (**1**) was synthesized according to ref 24 and dehydrated before use (10^{-5} Torr, 280 °C, 4 h, heating rate 1 °C min^{-1}). The IR spectra were recorded on a Perkin-Elmer 1600 series FTIR spectrometer and a Perkin-Elmer FTIR spectrometer 1760X using Nujol mulls between CsI plates. Solution NMR spectra were performed on a JEOL-JMN-GX 400 instrument (400 MHz, ^1H; 100.54 MHz, ^{13}C). All spectra were recorded in C_6D_6 at ambient temperature unless otherwise noted. Elemental analyses were performed on an Elementar VarioEL and an Emission-Spektrometer Plasma400 (Perkin-Elmer).

N_2 Adsorption/Desorption. Nitrogen physisorption measurements were performed on an ASAP 2010 volumetric adsorption apparatus (Micromeritics) at 77.4 K for relative pressures from 10^{-2} to 0.60 ($a_m(N_2, 77.4\ K) = 0.162\ nm^2$). Prior to analysis, the samples were outgassed at ambient temperature for 5 h under vacuum (about 10^{-3} Torr) unless otherwise noted in Table 4. The specific surface area a_S was determined by means of the Brunauer−Emmett−Teller method (eq 3; n^a = amount of nitrogen adsorbed at the relative pressure p/p_0, n^a_m = monolayer capacity, C = BET constant). The pore size

$$\frac{p}{n^a(p^0 - p)} = \frac{1}{n^a_m C} + \frac{(C-1)\,p}{n^a_m C\,p^0} \tag{3}$$

distribution was obtained on the basis of the Barret−Joyner−Halenda (BJH) method using the Kelvin equation (eq 4; r_K = Kelvin radius for cylindrical pore shape; σ^{lg} = surface tension of the liquid condensate; ν^l = molar volume of the liquid condensate; R = universal gas constant at the absolute temperature T) to calculate the mean pore diameter d_p (eq 5; t_{ads} = correction term for multilayer thickness).[30] The reproducibility of the measurements was controlled by a second run.

$$r_K = \frac{2\sigma^{lg}\nu^l}{RT\ln(p^0/p)} \tag{4}$$

$$d_p = 2(r_K + t_{ads}) \tag{5}$$

Magic-Angle Spinning Nuclear Magnetic Resonance Spectroscopy. MAS NMR experiments for ^1H, ^{13}C, and ^{27}Al were carried out at 400.13, 100.63, and 104.23 MHz, respectively, on a Bruker MSL-400 spectrometer equipped with a standard 4 mm MAS probe (^1H and ^{27}Al) or standard 7 mm MAS probe (^{13}C). Single-pulse excitation has been applied for the ^1H, ^{13}C, and ^{27}Al spectra, for the latter in combination with high-power proton decoupling. ^{27}Al NMR spectra were also measured under static conditions using a quadecho pulse sequence. ^{13}C MAS NMR spectra were also recorded using cross polarization. The following conditions were used in the measurements: ^1H, pulse repetition 5 s, $\pi/2$ pulse, spinning speed 10 kHz; ^{13}C, pulse repetition 15 s, $\pi/2$ pulse, spinning speed 3 kHz, CP contact time 5 ms; ^{27}Al, pulse repitition 0.5 s, $\pi/12$ pulse, spinning speed 8 kHz. ^1H and ^{13}C spectra were referenced to $Si(CH_3)_4$, and ^{27}Al spectra were referenced to a 1 M aqueous solution of $Al(NO_3)_3$.

General Procedure for the Chemisorption of $AlMe_3$ onto MCM-41 (1). $AlMe_3$ (*n* mmol/g of **1**; $n = 1-6, 10$), diluted with 2 mL of *n*-hexane, was added to a suspension of **1** (approximately 0.200 g) in 10 mL of *n*-hexane within a time period < 2 min at ambient temperature. The reaction mixture was stirred for 20 h at ambient temperature and then separated via centrifugation. The residue was washed several times with *n*-hexane (20 mL). The hybrid materials **9** were dried in vacuo for at least 5 h. The elemental analysis data are given in Table 1. ***Caution!*** The *n*-hexane fractions containing unreacted $AlMe_3$ react violently when exposed to air. The $AlMe_3$ should be deactivated inside the glovebox by addition of anhydrous alcohols such as ethanol.

Treatment of 2d with $HOC(CF_3)_3$. Perfluorinated alcohol (0.83 g, 3.52 mmol) diluted with 2 mL of THF was added via syringe to a suspension of **2e** (0.300 g, 1.15 mmol Al) in *n*-hexane within a time period of < 2 min at ambient temperature. The vial was sealed with Parafilm, and the reaction mixture was stirred for 48 h and then separated by centrifugation. The residue was washed several times with THF (20 mL), and the solvent was evaporated, leaving hybrid material **3a** (0.340 g). Subsequent treatment of **3a** at 250 °C/10^{-3} Torr for 3 h yielded **3b** (0.280 g; IR (ν(OH)/cm^{-1}) 3742−3568w (br)). The volatile components of the combined THF fractions were

(54) Maruoka, K.; Nagahara, S.; Yamamoto, H. *J. Am. Chem. Soc.* **1990**, *112*, 6115.
(55) Herrmann, W. A.; Anwander, R.; Munck, F. C.; Scherer, W.; Dufaud, V.; Huber, N. W.; Artus, G. R. J. *Z. Naturforsch.* **1994**, *49B*, 1789.

evaporated, leaving 0.200 g of a white crystalline solid which could be identified as an aluminum alkoxide by IR spectroscopy.

Treatment of 2e with Acetylacetone. Approximately 0.300 g (1.15 mmol Al) of **2e** was suspended in a mixture of acetylacetone (10 mL)/ethanol (35 mL) and stirred at 80 °C for 1 day. After centrifugation and separation, this procedure was repeated. Then the residue was washed several times with THF and treated at 250 °C/10^{-3} Torr for 3 h to yield material **4**. IR (ν(OH)/cm^{-1}): 3693−3570w (br), 3470w (br). Evaporation of the THF fractions yielded $Al(acac)_3$ as a white solid.

General Procedure for the Reaction of $Y[N(SiHMe_2)_2]_3(THF)_2$ (5) with $AlMe_3$-Modified MCM-41 (2). Compound **5** (0.152 g, 0.24 mmol), dissolved in 10 mL of *n*-hexane, was added to a suspension of **2d** and **2e** (0.597 g, 1.99 mmol of Al), respectively, in *n*-hexane within a time period of <2 min at ambient temperature. The reaction mixture was stirred for 20 h at ambient temperature and then separated via centrifugation. The residue was washed several times with *n*-hexane (20 mL), and the solvent was evaporated. The resulting hybrid materials **7** and **8** were dried in vacuo for at least 5 h. The *n*-hexane fractions were collected, and the solvent was evaporated. The resulting solid residues were identified by IR and NMR spectroscopy.

Products, obtained via **2d**. **7**: IR (ν/cm^{-1}) "$N(SiHMe_2)_2$" 2151m, 2085m, 899s, 836m, 678m, 626m. ICP Anal. Found: Y, 1.7. **6**: IR (cm^{-1}) 2072s, 1939 (sh), 1296w, 1243vs, 1072vs (br), 936vs, 896s, 835s, 787m, 761m, 675m, 619m, 606m, 404m. ^{1}H NMR: δ 4.92 (sept, 6H, SiH; ^1J(Si, H) = 161 Hz, ^3J(H,H) = 2.9 Hz), 3.78 (m, 4H, thf), 1.23 (m, 4H, thf), 0.36 (d, ^3J(H,H) = 2.9 Hz, 36H, $SiCH_3$). $^{13}C\{^1H\}$ NMR: δ 71.9 (thf), 25.2 (thf), 3.2 ($SiCH_3$). $AlMe_3$(THF): ^{1}H NMR −0.42.

Products, obtained via **2e**. **8**: IR (ν/cm^{-1}) No indication of a significant "$N(SiHMe_2)_2$" vibration mode. ICP Anal. Found: Y, 1.4. **6**: Compare with above. "$Y(AlMe_4)$": ^{1}H NMR δ −0.29. $\{\mu$-$[N(SiHMe_2)_2]AlMe_2\}_2$: IR (ν/cm^{-1}) 2183s. ^{1}H NMR: δ 5.02 (sept, ^1J(Si,H) = 211 Hz, ^3J(H,H) = 2.9 Hz, 1H, SiH), 0.20 (d, ^3J(H,H) = 2.9 Hz, 12H, $SiMe_2$), −0.12 (s, 6H, AlMe).

Acknowledgment. We thank the Deutsche Forschungsgemeinschaft for support, including a fellowship (to R.A.). Generous support from Prof. J. Weitkamp is gratefully acknowledged. We thank J. Eppinger for performing the solution NMR measurements.

OM9710632